Acid−Base Profiling of Imatinib (Gleevec) and Its Fragments

Zoltán Szakács,[†] Szabolcs Béni,[‡] Zoltán Varga,[§] László Örfi,[‡] György Kéri,[§,‖] and Béla Noszál*[,‡]

*Department of Inorganic and Analytical Chemistry, Loránd Eötvös University, Pázmány Péter sétány 1/a,
H-1117 Budapest, Hungary, Department of Pharmaceutical Chemistry, Semmelweis University, Högyes E.u. 9,
H-1092 Budapest, Hungary, Cooperative Research Center, Semmelweis University, POB 131,
H-1367 Budapest, Hungary, and Peptide Research Group of the Hungarian Academy of Sciences,
Department of Medical Chemistry, Semmelweis University, Puskin u. 9, H-1088 Budapest, Hungary*

The site-specific basicities of imatinib (Gleevec, a new signal transduction inhibitor drug of chronic myeloid leukemia) and two of its fragment compounds were quantitated in terms of protonation macroconstants, microconstants, and group constants by NMR−pH and pH-potentiometric titrations. Sequential protonation of imatinib follows the N^{34}, N^{11}, N^{31}, N^{13} order, in which N^{11} and N^{31} show commensurable basicity, but negligible intramolecular interaction. Fragment compounds include two "halves" of imatinib, and their moiety-specific basicities confirm the NMR-based protonation sequence of the parent compound. NMR−pH profiles, macro- and/or microscopic protonation schemes, and species-specific distribution diagrams are presented. On the basis of these data, imatinib is shown to be predominantly neutral, monocationic, and tricationic at intestinal, blood, and gastric pH, respectively. The molecular hypotheses on imatinib binding to the Bcr-Abl oncogene fusion protein are interpreted at the site-specific level in view of the moiety basicities of imatinib.

Introduction

Imatinib mesylate (Gleevec, 4-(4-methyl-piperazin-1-ylmethyl)-*N*-[4-methyl-3-(4-pyridin-3-yl-pyrimidin-2-ylamino)-phenyl]-benzamide methanesulfonate) is indicated for the treatment of chronic myeloid leukemia (CML) and unresectable and/or metastatic malignant gastrointestinal stromal tumors (GIST).[1] CML is a clonal hematopoietic stem cell disorder characterized by the presence of the Philadelphia chromosome. A hallmark of this leukemia is a reciprocal chromosomal translocation involving the bcr gene from chromosome 9 and the c-abl gene from chromosome 22. The resulting Bcr-Abl fusion proteins have elevated nonreceptor tyrosine kinase catalytic activity, causing cell transformations and the concomitant malignancy.[2] The most potent, selective inhibitor of Bcr-Abl is imatinib, signal transduction inhibitor 571 (STI 571). This ATP mimic drug has a high affinity for Abl kinase, while being essentially inactive against Ser/Thr-kinases and most of the tyrosine kinases.[3,4]

In spite of its enormous therapeutic importance, the main physicochemical properties of imatinib have not been reported. The only data on its acid−base properties are based on pH-dependent capillary zone electrophoresis,[5] claiming that protonation of the neutral imatinib **1** starts below pH 5, but providing no quantitative parameters. Considering the protonation constants of *N*-methylpiperazine[6] (log K = 9.85), the lack of proton binding of **1** above pH 5 is highly unlikely.

Here we report the site-specific acid−base properties of imatinib. In order to quantitate the basicity of

* Corresponding author. Phone: (36) 1 2170891. Fax: (36) 1 2170891. E-mail: nosbel@hogyes.sote.hu.
† Loránd Eötvös University.
‡ Department of Pharmaceutical Chemistry, Semmelweis University.
§ Cooperative Research Center, Semmelweis University.
‖ Department of Medical Chemistry, Semmelweis University.

imatinib, we combined pH-potentiometry with NMR−pH titrations. The same methodology plus UV−pH titrations were applied to characterize two fragment compounds, 4-methyl-*N*-3-(4-pyridin-3-yl-pyrimidin-2-yl)-benzene-1,3-diamine **2** and 4-(4-methyl-piperazin-1-ylmethyl)-benzamide **3** (for structures and numbering, see Figure 1). **2** is also known to be a pharmaceutical impurity of Gleevec.[7] Potentiometric titrations provided the protonation constants in the range 2 < log K_i < 12. To define the loci for the potentiometric results and to determine the protonation constants in highly acidic pH, ¹H NMR−pH titrations were carried out for all ligands. Analysis of the NMR−pH profiles allowed a site-specific insight into the alternative protonation pathways in **1** and **2**. In particular, the intrinsic basicity of the pyridyl and piperazinyl nitrogens of **2** have been characterized in terms of microscopic protonation constants, while for imatinib **1** the main route of protonation could be identified.

Results and Discussion

Potentiometric Titrations. Potentiometric titration curves were transformed into Bjerrum plots (Figure 2), which show the mean number of protons associated with one ligand molecule at any arbitrary pH. In the pH interval 2 through 12, three protonation steps are observed for imatinib **1**, while both **2** and **3** bind two protons. The resulting protonation constants are summarized in Table 1. The outstanding uncertainty of log K_1 = 7.7 of **1** is due to ligand precipitation above pH 6.5 even at 1 mM concentration. Aqueous solvent mixtures such as 65% (w/w) DMSO or 40% (w/w) methanol eliminate the solubility problem, but they heavily modify the equilibria. Similar precipitation occurred for **2** at concentrations >3 mM above pH 7. The fact that a log K_1 value about 8 has been determined for both **1** and **3** but not for **2** confirms that the *N*-methyl
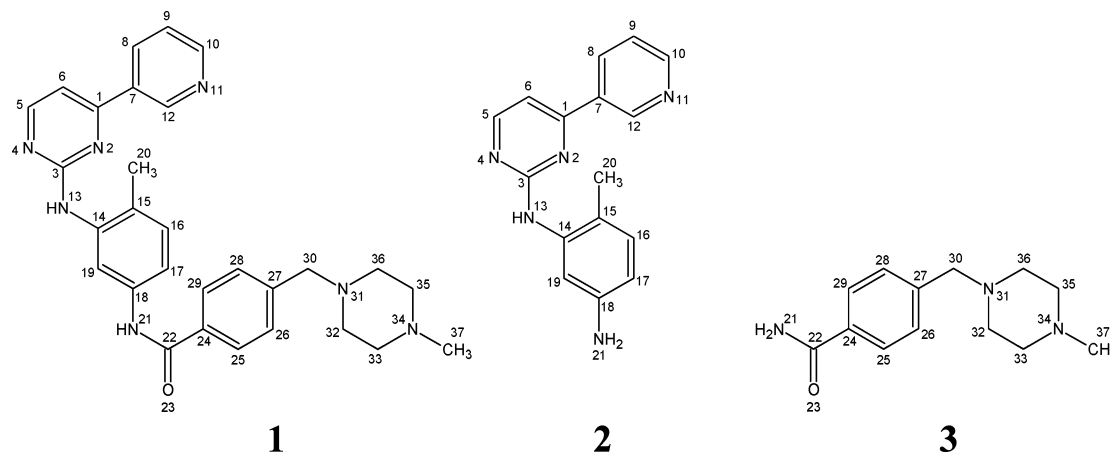
Figure 1. Structure and numbering of the compounds studied (for systematic names, see text). For comparison, the numbering of imatinib **1** is retained for the corresponding atoms of **2** and **3**.
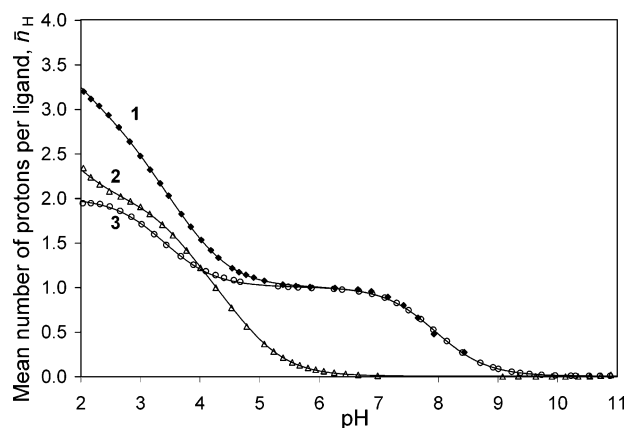

Figure 2. Bjerrum plots from the potentiometric titrations of **1**, **2**, and **3**. Computer fits are shown in solid lines.

Table 1. Macroscopic Protonation Constants in H_2O at 25 °C, I = 0.15 M (NaCl), Determined by Potentiometric (and in Part by ^{1}H NMR) Titrations

compd	$\log K_1$	$\log K_2$	$\log K_3$	$\log K_4$
1	7.7 ± 0.1^a	3.88 ± 0.03	3.10 ± 0.01	$1.71^b \pm 0.02$
2	4.75 ± 0.01	3.72 ± 0.01	$1.16^b \pm 0.03$	
3	7.95 ± 0.01	3.37 ± 0.02		

^{a} Uncertainties are estimates of standard deviation (1σ values). ^{b} Determined by ^{1}H NMR−pH titration.

piperazinyl nitrogen is the binding site in the weakly basic pH range.

The protonation at pH < 2 cannot be accurately studied by potentiometric titrations due to experimental difficulties involving the large buffering capacity of solvent water and the non-Nernstian response of the glass electrode. However, NMR titrations do not suffer from these limitations and reveal an additional protonation step at pH < 2 for both **1** and **2** (see below).

NMR-pH Titration of 3. The aromatic part of the ^{1}H NMR spectrum of **3** contains the characteristic AA′BB′ multiplet of the *para*-disubstituted phenyl ring. The nonequivalent amide protons give rise to two broad singlets near 8.1 and 7.3 ppm at pH < 7. These signals disappear in alkaline solutions as the rate of base-catalyzed amide proton exchange increases. In the aliphatic region, the piperazinyl methylenes show two exchange-broadened peaks due to the conformational dynamics of the piperazine ring, which collapse to a single, broad resonance at pH extremes.
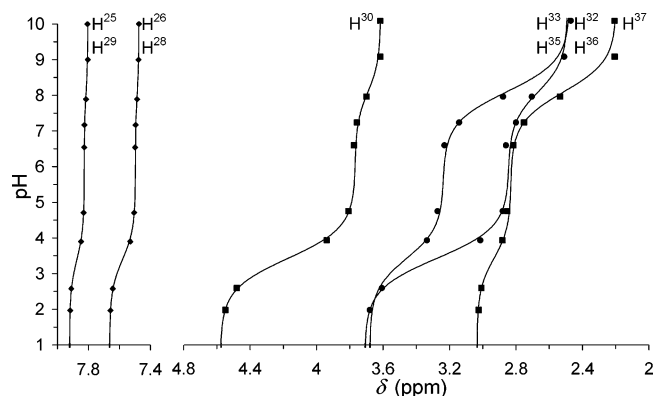

Figure 3. ^{1}H NMR−pH titration curves of **3**, with computer fits in solid lines.

The pH-dependent chemical shifts of all carbon-bound protons are depicted in Figure 3. Since protonation processes are rapid on the NMR time scale, the observed chemical shifts (δ^{obs}) are weighted averages[8] of those of the distinct protonation forms (δ_L, δ_{HL^+}, and $\delta_{H_2L^{2+}}$):

$$\delta^{obs} = \delta_L x_L + \delta_{HL^+} x_{HL^+} + \delta_{H_2L^{2+}} x_{H_2L^{2+}} \quad (1)$$

Expressing the x mole fractions in terms of pH and logarithms of K protonation constants, the master equation to fit the NMR−pH titration curves is obtained:

$$\delta^{obs} = \frac{\delta_L + \delta_{HL^+}(10^{\log K_1 - pH}) + \delta_{H_2L^{2+}}(10^{\log K_1 + \log K_2 - 2pH})}{1 + 10^{\log K_1 - pH} + 10^{\log K_1 + \log K_2 - 2pH}} \quad (2)$$

Equation 2 holds separately for each nucleus. The log K values obtained by potentiometry are used to determine the individual chemical shifts δ_L, δ_{HL^+}, and $\delta_{H_2L^{2+}}$ by parameter estimation, and the results are collected in Table S1 of the Supporting Information. The protonation shifts $\Delta_0^1\delta = \delta_{HL^+} - \delta_L$ and $\Delta_1^2\delta = \delta_{H_2L^{2+}} - \delta_{HL^+}$ hold information on the protonation sequence of the molecule.

All NMR−pH titration curves exhibit inflections near the log K values. The protonation shifts in ^{1}H NMR spectroscopy are greatest for nuclei in the vicinity of the basic site.[9] Upon coordination of the first proton to N^{34} with log $K_1 = 7.95$, the greatest effects are observed at the piperazinyl H^{33}/H^{35} nuclei (0.76 ppm) and the
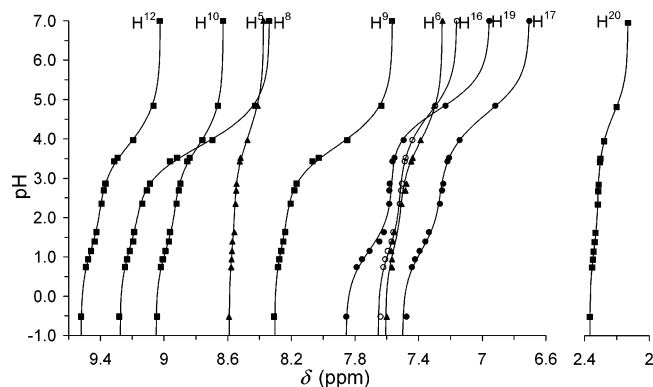
Figure 4. ¹H NMR−pH titration curves of **2**, with computer fits in solid lines.

N-methyl H³⁷ ($\Delta_0^1\delta = 0.63$ ppm). Protonation of N³¹ with log $K_2 = 3.37$ is monitored most sensitively by the nearby H³⁰ and H³²/H³⁶ methylenes, with downfield shifts of $\Delta_1^2\delta = 0.81$ and 0.87 ppm, respectively.

NMR−pH Titration of 2. The multiplets in the aromatic part of the ¹H NMR spectrum of **2** exhibit mostly first-order pattern even at 250 MHz. Figure 4 shows the chemical shifts of the carbon-bound protons as functions of pH. The NMR−pH datasets were fitted by the following, triprotic extension of eq 2:

$$\delta^{obs} = [\delta_L + \delta_{HL^+}(10^{\log K_1 - pH}) + \delta_{H_2L_{2+}}(10^{\log K_1 + \log K_2 - 2pH}) +$$
$$\delta_{H_3L^{3+}}(10^{\log K_1 + \log K_2 + \log K_3 - 3pH})]/[1 + 10^{\log K_1 - pH} +$$
$$10^{\log K_1 + \log K_2 - 2pH} + 10^{\log K_1 + \log K_2 + \log K_3 - 3pH}] \quad (3)$$

This calculation yielded the chemical shifts of the individual H_iL^{i+} species (Table S2, Supporting Information) and the value of the third protonation constant log $K_3 = 1.16$, which could not be obtained by potentiometry.

All NMR−pH profiles in Figure 4 show two steps. The large downfield shift occurs in the pH interval 6 to 2.3 and reflects the coordination of the first two protons. The $\Delta\delta$ protonation shifts in Table S2 hold useful information to identify these two protonation sites. The first protonation occurs mainly at the N²¹ amine group, as H¹⁹, H¹⁷, and H¹⁶ of the phenyl ring are most affected. The largest $\Delta_1^2\delta$ values are observed at H⁸, H⁹, H¹⁰, and H¹², indicating the protonation of the pyridyl nitrogen N¹¹. Although the main protonation pathway is N²¹ → N¹¹, the alternative N¹¹ → N²¹ protonation pathway cannot be neglected either. Because of overlap in the two protonation steps, log K_1 and log K_2 are not direct measures of the pyridyl (P) and amine (N) basicity. The exact, site-specific characterization takes the microscopic protonation scheme (Figure 5). This treatment distinguishes between the protonation isomers (microspecies) denoted by P and N that have the same overall composition HL⁺. The four microscopic protonation constants, k^N, k^P, k_P^N, k_N^P, characterize the basicity of the P and N sites directly. In order to determine these constants, "reporter" nuclei were chosen to selectively monitor the protonation of each group through their chemical shifts. The aromatic protons of the pyridyl ring are separated by more than 9 bonds from the N²¹ amine group, so any of them can well be assumed to be a selective indicator of the N¹¹ protonation. Using the chemical shift−pH profile of H⁹, the f_P
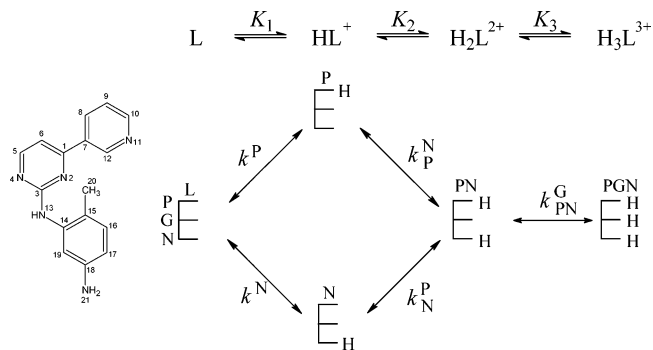

Figure 5. Macroscopic and microscopic protonation scheme of **2**. P, G, and N represent the pyridyl N¹¹, the guanidine N¹³, and the amine N²¹ nitrogens, while K and k denote macroscopic and microscopic protonation constants, respectively.

protonation fraction of the pyridyl nitrogen can be obtained, which enables the calculation of k^P, one of the unknown microconstants, by fitting the following function:

$$f_P = \frac{\delta_{H^9}^{obs} - \delta_{L,H^9}}{\delta_{H_2L,H^9} - \delta_{L,H^9}} = \frac{10^{\log k^P - pH} + 10^{\log K_1 + \log K_2 - 2pH}}{1 + 10^{\log K_1 - pH} + 10^{\log K_1 + \log K_2 - 2pH}} \quad (4)$$

Thus, a log $k^P = 4.07$ value was obtained. Since the K macroconstants are known from potentiometry, the knowledge of log k^P allows the calculation of the other three microconstants (Table 2), using the relationships between micro- and macroconstants.[9,10] Microconstants differing by 0.01 unit were obtained when the evaluation was repeated for nuclei H⁸ or H¹⁰.

As a further check of the consistency of the microconstant set, similar calculations were carried out to obtain k^N from the NMR titration curve of each "amine reporter" nuclei H¹⁶, H¹⁷, and H¹⁹, resulting in log k^N values of 4.64, 4.65, and 4.71, respectively.

Interaction between sites N and P can be quantified in terms of log k^P − log k_N^P = log k^N − log k_P^N, the interactivity parameter. Its 0.25 value in log units indicates that these sites are in weak interactions in **2**, which is, however, irrelevant in the parent compound where N²¹ exists in amide bond, bearing thus no basicity in this pH range.

NMR−pH Titration of Imatinib 1. The ¹H NMR titration of 3 mM imatinib **1** was restricted to the pH < 6 range to avoid precipitation. The piperazine methylenes appear in broad signals between 3 and 4 ppm, so these peaks were omitted from the analysis. The chemical shifts of other carbon-bound hydrogens are plotted as functions of pH in Figure 6. By evaluation of these curves, the first protonation step of **1** was disregarded and the coordination of three protons to HL⁺ was considered. Using K_2 and K_3 from potentiometry, eq 3 was fitted to all NMR−pH datasets simultaneously to obtain log $K_4 = 1.71$ and the chemical shifts of the individual H_iL species (Table S3, Supporting Information). The $\Delta\delta$ protonation shifts help to identify the protonation pattern of **1**.

Figure 7 shows the protonation scheme of **1**. Once the first proton to the piperazinyl N³⁴ (labeled as group A) is attached, two alternative pathways occur, leading either to the N¹¹-protonated microspecies PA or to the N³¹-protonated one, labeled here as AB. To determine
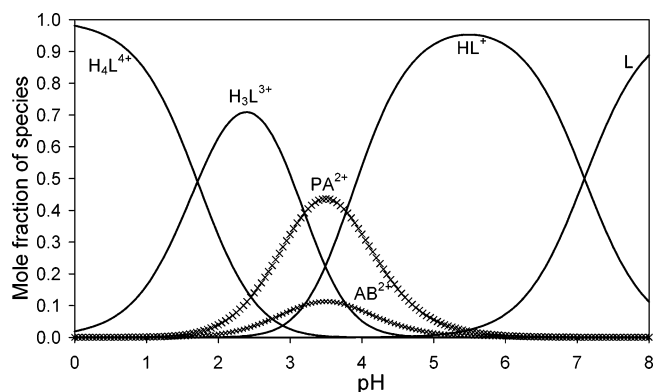
Table 2. Microscopic Protonation Constants of **1** and **2**, Determined by ^{1}H NMR−pH Titration ($T = 25$ °C, $I = 0.15$ M with NaCl, Solvent H_2O)[a]

compd	N[11]		N[31] in **1** and N[21] in **2**		N[13]	
1	$\log k_A^P$	3.78 ± 0.02	$\log k_A^B$	3.20 ± 0.02	$\log k_{PAB}^G$	1.71 ± 0.02
	$\log k_{AB}^P$	3.78 ± 0.02	$\log k_{PA}^B$	3.20 ± 0.02		
2	$\log k^P$	4.07 ± 0.04	$\log k^N$	4.65 ± 0.01	$\log k_{PN}^G$	1.16 ± 0.03
	$\log k_N^P$	3.82 ± 0.02	$\log k_P^N$	4.40 ± 0.04		

[a] See Figures 5 and 6 to assign microconstants.
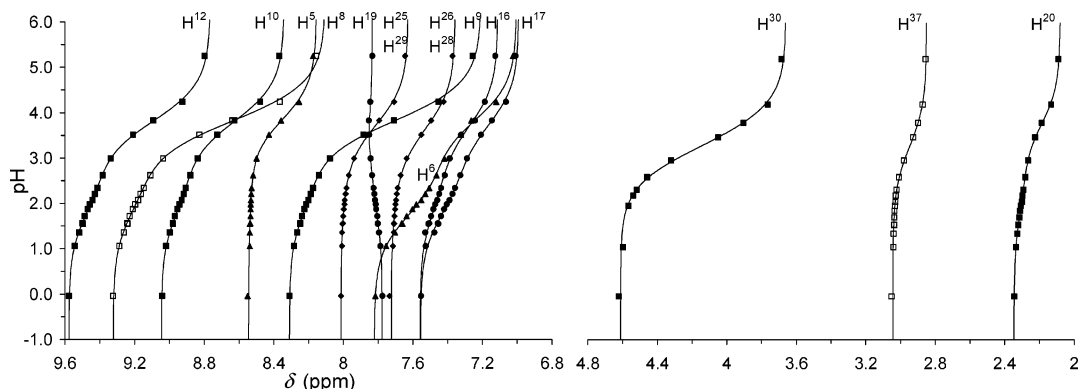
Figure 6. ^{1}H NMR−pH titration curves of imatinib **1**, with computer fits in solid lines.
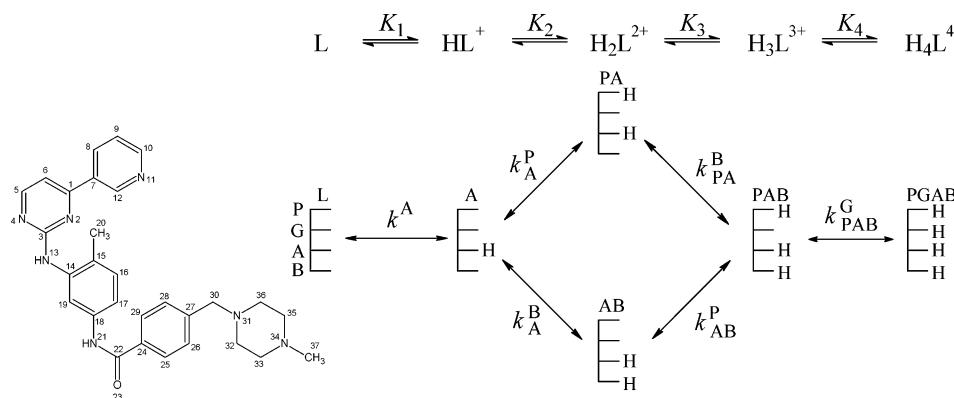
Figure 7. Macroscopic and microscopic protonation scheme of imatinib **1**. P, G, A, and B represent the pyridyl N[11], the guanidine N[13], and the piperazine N[34] and N[31] nitrogens, while K and k denote macroscopic and microscopic protonation constants, respectively.

the microconstant k_A^P, H[10] was chosen as protonation sensor for the pyridyl N[11] (labeled as P). With the calculation outlined above, the microconstants in Table 2 were obtained and similar results are gained from the NMR−pH titration curve of H[12]. The microconstants indicate that the pyridyl nitrogen is 3.8 times more basic than N[31]. Two pairs of microconstants, referring to the same group, are equal. This fact indicates that the protonation of one site does not diminish appreciably the basicity of the other one, which is, in principle, an example of the group constant approximation.[10] This independence of groups indicates not only the long covalent distance between N[11] and N[31] but also the rigidity of imatinib, since flexible molecules of similar intermoiety distance show 0.2−0.3 interactivity in log k units.[12]

The last protonation of **1** occurs at N[13]. Accordingly, the corresponding microconstant log k_{PAB}^G practically equals log $K_4 = 1.71$. The value of this constant clearly shows that this moiety is a 2-amino-pyrimidine structure rather than formally resembling a guanidino unit.

Figure 8. Distribution curves of the macrospecies (H_iL) and microspecies (PA and AB) of imatinib **1**.

The macroscopic and microscopic protonation constants enable the calculation of the species distribution of **1** (Figure 8) in compartments of various pH of the human body. In the blood (pH 7.4), 33% of imatinib is monocationic (HL[+]), holding the single proton on the piperazine A site. At the duodenal pH of 4.6, 80% of

imatinib is monocationic, while the remaining fraction is present in the form of two dicationic (H_2L^{2+}) protonation isomers. In the stomach (pH 2), the tricationic H_3L^{3+} (63%) and the fully protonated H_4L^{4+} (33%) are the most abundant species.

Conclusion

Several hypotheses were reported on the possible electrostatic and H-bonding contact points between imatinib and the complementary Bcr-Abl oncogene.[2−4] In the model of Corbin et al.,[3] a hydrogen bond is assumed between N^{34} of imatinib and Glu^{258} in the ATP binding pocket of the active form of the Abl kinase domain. This interaction is supported by the protonation constant of N^{34} (log K = 7.7), which makes N^{34} the most basic site of imatinib and facilitates its proton-donor role in such bindings. In the binding pattern, the role of the pyridyl N^{11} atom is barely understood. In the crystal structure of the Abl catalytic domain with a variant of imatinib, N^{11} was described[2] as an acceptor in its unprotonated form for an H-bond with the Met^{318} peptide group in the unprotonated form. Similarly, the guanidino N^{13} atom is assumed[2,4] to be a proton acceptor in an H-bond from Thr^{315}. The condition of this H-bond, the unprotonated state of N^{13}, is certainly met in view of our log K = 1.71 data, indicating that N^{13} is basic, but largely unprotonated under all physiological circumstances, accommodating thus proton donor moieties of counter molecules.

Experimental Section

Materials. The free bases of **1**, **2**, and **3** were synthesized as detailed in the following section. Other base chemicals of analytical grade were purchased from commercial suppliers and used without further purification. All solutions were prepared from bidistilled Millipore water (conductivity: 1.1 μS cm^{-1}).

Synthetic Chemistry. General Experimental Procedures. All reagents and solvents were obtained from Sigma-Aldrich Co. and used without purification and drying. Melting points were determined with a MEL-TEMP capillary melting point apparatus and are uncorrected. Synthesis-supporting ^1H NMR spectra were recorded using a Bruker Avance DRX 300 MHz spectrometer. Chemical shifts are given in parts per million relative to TMS. Electrospray ionization mass spectra were recorded on a Waters 2795 HPLC, equipped with a Waters 996 photodiode array detector and a Micromass ZMD 2000 LC−MS system. Retention factors were determined on silica gel G$_{F254}$ TLC plates eluting with mixture of chloroform/methanol 10/1. The purity of the compounds was also checked in two RP-HPLC systems, using an acetonitrile/water gradient (HPLC1) and a methanol/water gradient (HPLC2); other relevant parameters are listed in Table S5 of the Supporting Information).

4-(4-Methyl-piperazin-1-ylmethyl)-benzamide (3). 4-Chloromethyl-benzoyl chloride (378 mg, 2 mmol) was dissolved in 50 cm^3 of tetrahydrofuran and cooled to 0 °C. Concentrated ammonia solution (0.27 cm^3, 4 mmol) was added slowly to the cold solution. The reaction mixture was vigorously stirred for 10 min at 0 °C, and then the mixture was poured on 50 cm^3 of ice water. The aqueous layer was extracted three times with 50 cm^3 of ethyl acetate. The combined organic layers were dried over magnesium sulfate and evaporated to dryness. Acetonitrile (20 cm^3) and 1.11 cm^3 (10 mmol) of N-methylpiperazine were added to the residue, and the reaction mixture was refluxed for 4 h. Then the reaction mixture was cooled to 0 °C. Crystalline **3** (292 mg, 63%) was filtered off after 1 h. Anal. (C$_{13}$H$_{19}$N$_3$O) C calcd, 66.92; found, 64.84; H calcd, 8.21; found, 7.55; N calcd, 18.01; found, 17.34. Mp: 156−159 °C. R_f

= 0.1 (chloroform:methanol = 10:1; retention times: 2.54 min (HPLC1) and 2.45 min (HPLC2). MS: (M + H)$^+$ = 234. ^1H NMR (DMSO-d_6, 300 MHz) δ (ppm): 7.91 (bs, 1H, NH$_{2\alpha}$), 7.81 (d, 2H, ^3J = 8.2 Hz), 7.35 (d, 2H, ^3J = 8.1 Hz), 7.30 (bs, 1H, NH$_{2\beta}$), 3.48 (s, 2H, CH$_2$), 2.34 (bs, 8H), 2.14 (s, 3H, CH$_3$).

4-Methyl-N-3-(4-pyridin-3-yl-pyrimidin-2-yl)-benzene-1,3-diamine (2). 3-Acetylpyridine (64.1 cm^3, 583 mmol) and 94.0 cm^3 (700 mmol) of N,N-dimethyl-formamide dimethyl-acetal were refluxed in 250 cm^3 of ethyl alcohol overnight. The reaction mixture was evaporated under reduced pressure, 100 cm^3 of diethyl ether was added to the residue, and the reaction mixture was cooled to 0 °C. 3-Dimethylamino-1-pyridin-3-yl-propenone (71.2 g) was filtered off as yellow crystals. (Yield: 69%.) This material was used in the subsequent steps without further purification.

2-Methyl-5-nitro aniline (22.8 g, 150 mmol) was dissolved in 60 cm^3 of ethyl alcohol, and 10.5 cm^3 of concentrated HNO$_3$ was added to the solution dropwise followed by 25.2 cm^3 (300 mmol) of a 50% aqueous solution of cyanamide. The reaction mixture was refluxed overnight and then cooled to 0 °C. N-(2-Methyl-5-nitro-phenyl)-guanidinium nitrate (20.6 g) was filtered off and washed well with ethyl acetate and diethyl ether. (Yield: 53%.)

To a suspension of 26.4 g (150 mmol) of 3-dimethylamino-1-pyridin-3-yl-propenone and 40.8 g (157.5 mmol) of N-(2-methyl-5-nitro-phenyl)-guanidinium nitrate in 220 cm^3 of 2-propanol was added 6.95 g (175 mmol) of NaOH. The reaction mixture was refluxed for 24 h. Then it was cooled to 0 °C. The precipitate was filtered off, suspended in water, filtered off again, and finally washed with 2-propanol and diethyl ether. This reaction gave 30.1 g of (2-methyl-5-nitro-phenyl)-(4-pyridin-3-yl-pyrimidin-2-yl)-amine. (Yield: 65%.)

A solution of 42 g (186 mmol) of SnCl$_2$·2 H$_2$O in 115 cm^3 of concentrated hydrochloric acid was added to 12.3 g (40 mmol) of (2-methyl-5-nitro-phenyl)-(4-pyridin-3-yl-pyrimidin-2-yl)-amine while the suspension was vigorously stirred. After 30 min of stirring the mixture was poured onto crushed ice, made alkaline with K$_2$CO$_3$, and extracted three times with 100 cm^3 of ethyl acetate. Organic phases were combined, dried over MgSO$_4$, and evaporated to dryness. Recrystallization from dichloromethane resulted in 8.9 g of **2** (yield: 81%) as an off-white solid. Anal. (C$_{15}$H$_{15}$N$_5$) C; N calcd, 5.45; found, 6.16; N calcd, 25.25; found, 19.48. Mp: 134−136 °C. R_f = 0.5 (chloroform:methanol = 10:1), retention times: 3.64 min (HPLC1) and 4.62 min (HPLC2). MS: (M + H)$^+$ = 278. ^1H NMR (DMSO-d_6, 300 MHz) δ (ppm): 9.22 (s, 1H, NH), 8.67 (d, 1H, ^3J = 4.4 Hz), 8.63 (s, 1H), 8.44 (d, 1H, ^3J = 5.1 Hz), 8.39 (d, 1H, ^3J = 8.0 Hz), 7.51 (dd, 1H, ^3J = 7.9 Hz, ^4J = 4.8 Hz), 6.85 (d, 1H, ^3J = 8.0 Hz), 6.77 (d, 1H, ^4J = 1.4 Hz), 6.32 (dd, 1H, ^3J = 8.0 Hz, ^4J = 2.0 Hz), 4.80 (s, 2H, NH$_2$), 2.04 (s, 3H, CH$_3$).

4-(4-Methyl-piperazin-1-ylmethyl)-N-[4-methyl-3-(4-pyridin-3-yl-pyrimidin-2-ylamino)-phenyl]-benzamide (1). 4-Methyl-N-3-(4-pyridin-3-yl-pyrimidin-2-yl)-benzene-1,3-diamine (3.3 g, 12 mmol) was dissolved in 150 cm^3 of N,N-dimethylformamide and cooled to 0 °C. Then 3.4 g (18 mmol) of 4-chloromethylbenzoyl chloride was added. The reaction mixture was stirred for 2 h before it was poured onto 500 g of crushed ice. This mixture was neutralized with NaHCO$_3$ and stirred for an hour. The precipitate was filtered off and recrystallized from ethyl alcohol, providing 3.1 g of 4-chloromethyl-N-[4-methyl-3-(4-pyridin-3-yl-pyrimidin-2-ylamino)-phenyl]-benzamide (yield: 61%) as a yellowish solid. 4-Chloromethyl-N-[4-methyl-3-(4-pyridin-3-yl-pyrimidin-2-yl-amino)-phenyl]-benzamide (1.6 g, 3.8 mmol) and 4.3 mL (38 mmol) of N-methyl piperazine were added to 150 cm^3 of acetonitrile. The reaction mixture was heated under reflux for 6 h, then evaporated to 50 cm^3, and cooled to 0 °C. The precipitate was filtered off and recrystallized from acetonitrile to provide 1.25 g (yield: 68%) of **1** as creamy white crystals. Anal. (C$_{29}$H$_{31}$N$_7$O) C calcd, 70.56; found, 69.03; H calcd, 6.33; found, 5.51; N calcd, 19.86; found, 25.14. Mp: 206−209 °C. R_f = 0.15 (chloroform:methanol = 10:1), retention times: 3.24 min (HPLC1) and 4.48 min (HPLC2). MS: (M + H)$^+$ = 494, (M − H)$^-$ = 492. ^1H NMR (DMSO-d_6, 300 MHz) δ (ppm): 10.14 (s, 1H, NH), 9.27 (d, 1H, ^4J = 1.8

Hz), 8.95 (s, 1H, NH), 8.68 (dd, 1H, $^3J = 4.7$ Hz, $^4J = 1.5$ Hz), 8.50 (d, 1H, $^3J = 6.9$ Hz), 8.49 (m, 1H), 8.08 (d, 1H, $^4J = 1.9$ Hz), 7.90 (d, 2H, $^3J = 8.2$ Hz), 7.54−7.41 (m, 5H), 7.20 (d, 1H, $^3J = 8.34$ Hz), 3.52 (s, 2H), 2.35 (bs, 8H), 2.22 (s, 3H, CH$_3$), 2.15 (s, 3H, CH$_3$).

Potentiometric Titrations. pH-metric titrations were carried out at 25.0 ± 0.1 °C. A Metrohm 716 DMS Titrino autoburet (Metrohm, Switzerland) equipped with a Metrohm 6.0234.110 combined glass electrode was used. The electrode system was calibrated in terms of hydrogen ion concentration[11] by titrating 2 mL of 0.05 M HCl with standardized 0.05 M NaOH. Both stock solutions contained calculated amounts of NaCl to ensure a constant ionic strength of 0.15 M during titration. For protonation constant determinations, a weighed amount of the ligand was dissolved in the HCl stock solution and titrated with NaOH. Measurements were performed at various ligand concentrations, 1−5 mM for **1** and **2** and 2−10 mM for **3**.

All titration curves were evaluated by our nonlinear least-squares regression program PROTC.[12] The acid−base chemistry of imatinib, a tetravalent base, is characterized in terms of log K protonation constants, although the term pK_a, the well-known acid dissociation parameter, is certainly widespread in medicinal and pharmaceutical chemistry. In order to comply with data in Critical Stability Constants,[13] "stoichiometric" protonation constants containing hydrogen ion concentration were calculated. To get "practical" protonation constants involving hydrogen ion activity, the log K values reported here should be increased by 0.12 unit.

^{1}H NMR Titrations with in Situ pH Monitoring. To acquire a pH-dependent series of ^{1}H NMR spectra, the recently developed[14] electrodeless single tube NMR titration was applied. In this method, titration of the ligand is carried out in a single NMR tube, which contains also pH-monitoring indicator molecules (dichloroacetic acid, chloroacetic acid, acetic acid, and tris(hydroxymethyl)aminomethane [TRIS]), the chemical shift of which show the actual pH after each titrant addition.

A single NMR sample solution of 0.7 mL was prepared, which contained 3 mM imatinib **1**, the indicators listed above (2 mM each), 0.05 M HCl to set the starting pH to 1.7, 1 mM sodium 3-(trimethylsilyl)-1-propanesulfonate (DSS) as internal chemical shift reference, and 0.096 M NaCl to give a total ionic strength of 0.15 M. After recording the ^{1}H NMR spectrum of this sample on a 500 MHz Varian Unity spectrometer, the sample tube was ejected and a small (3−20 μL) portion of an alkaline titrant solution (0.11 M NaOH, 0.12 M NaCl) was added from a medical syringe. After the contents of the NMR tube were homogenized, a new spectrum was acquired. Since the solution contained no D$_2$O, all ^{1}H spectra were measured without spectrometer lock at 25 °C and the resonance of solvent H$_2$O was diminished by a selective presaturation pulse before the observation pulse.[19] The NMR titrations of **2** and **3** were performed analogously on a 250 MHz Bruker Avance DRX spectrometer.

The freeware program Mestre-C[15] was used for spectral processing, followed by first-order multiplet analysis. ^{1}H chemical shifts are referenced to internal DSS, which does not alter its peak position even under strongly acidic circumstances.[16,20]

The pH belonging to each spectrum was determined from the actual chemical shift of the appropriate indicator δ_{Ind}^{obs}, using a rearranged form of the Henderson-Hasselbach equation:

$$pH = \log K_{Ind} + \log \frac{[Ind]}{[HInd]} = \log K_{Ind} + \log \frac{\delta_{Ind}^{obs} - \delta_{HInd}}{\delta_{Ind} - \delta_{Ind}^{obs}}$$

(5)

The log K_{Ind} protonation constants were determined in separate potentiometric titrations, and the results in Table S4 (Supporting Information) show a good agreement with literature values. The limiting chemical shifts δ_{Ind} and δ_{HInd} refer to the unprotonated and protonated forms of the indicator, respectively. These values are obtained from NMR spectra

of sufficiently basic or acidic solutions, respectively (Table S4). A special approach was necessary for dichloroacetate, where complete protonation could not be reached even at pH 0. In this case, the indicator parameters log $K = 1.06 \pm 0.01$ and $\delta_{HInd} = 6.328$ ppm were determined in a separate ^{1}H NMR titration at 1 M ionic strength.[16] The protonation constant was converted to 0.15 M ionic strength by the Davies equation[17] to yield log $K = 1.14$, while δ_{HInd} was converted empirically to 0.15 M ionic strength.

An important criterion of using in situ pH indicators is the lack of their interaction with other molecules in the sample. Since the δ_{Ind} and δ_{HInd} values of the same indicator vary from one NMR titration to another within the experimental error (ca. 0.002 ppm), such disturbing interferences are assumed to be negligible.

The NMR−pH datasets were evaluated with the OPIUM computer program.[18] For microconstant calculations, in-house least-squares C++ programs[12] were used.

Supporting Information Available: Tables S1, S2, and S3 displaying ^{1}H NMR chemical shifts [ppm] of individual H$_i$L species of **3**, **2**, and **1**, respectively, and their changes upon protonation. Table S4 displaying protonation constants, pH ranges, and limiting ^{1}H NMR chemical shifts [ppm] of the NMR−pH indicator molecules. Table S5 displaying summary of experimental data confirming the identity and purity of compounds **1**−**3**. This material is available free of charge via the Internet at http://pubs.acs.org.

References

(1) Levitzky, A. Signal Transduction Therapy. In *Molecular Pathomechanism and New Trends in Drug Research*, 1st ed.; Kéri, Gy., Tóth, I., Eds.; Taylor & Francis: New York, 2003; pp 55−58.
(2) Schindler, T.; Bornmann, W.; Pellicena, P.; Miller, W. T.; Clarkson, B.; Kuriyan, J. Structural Mechanism for STI-571 Inhibition of Abelson Tyrosine Kinase. *Science* **2000**, *289*, 1938−1942.
(3) Corbin, A. S.; Buchdunger, E.; Pascal, F.; Druker, B. J. Analysis of the Structural Basis of Specificity Inhibition of the Abl Kinase by STI571. *J. Biol. Chem.* **2002**, *277*, 32214−32219.
(4) Noble, M. E. M.; Endicott, J. A.; Johnson, L. N. Protein Kinase Inhibitors: Insights into Drug Design from Structure. *Science* **2004**, *303*, 1800−1805.
(5) Rodríguez Flores, J.; Berzas, J. J.; Castaneda, G.; Rodríguez, N. Direct and Fast Capillary Zone Electrophoretic Method for the Determination of Gleevec and its Main Metabolite in Human Urine. *J. Chromatogr., B* **2003**, *794*, 381−388.
(6) Frenna, V.; Vivona, N.; Consiglio, G.; Spinelli, D. Amine Basicities in Benzene and in Water. *J. Chem. Soc., Perkin Trans. 2* **1985**, *12*, 1865−1868.
(7) Vivekanand, V. V.; Rao, D. S.; Vaidynathan, G.; Sekhar, N. M.; Kelkar, S. A.; Puranik, P. R. Validated LC Method for Imatinib Mesylate. *J. Pharm. Biomed. Anal.* **2003**, *33*, 879−889.
(8) Jaroszewski, J. W.; Matzen, L.; Frolund, B.; Krogsgaard-Larsen, P. Neuroactive Polyamine Wasp Toxins: Nuclear Magnetic Resonance Spectroscopic Analysis of the Protolytic Properties of Philanthotoxin-343. *J. Med. Chem.* **1996**, *39*, 515−521.
(9) Szakács, Z.; Kraszni, M.; Noszál, B. Determination of Microscopic Acid-Base Parameters from NMR-pH Titrations. *Anal. Bioanal. Chem.* **2004**, *378*, 1428−1448.
(10) Noszál, B. Group Constant: A Measure of Submolecular Basicity. *J. Phys. Chem.* **1986**, *90*, 4104−4110.
(11) Irving, H. M.; Miles, M. G.; Pettit, L. D. A Study of Some Problems in Determining the Stoichiometric Proton Dissociation Constants of Complexes by Potentiometric Titrations Using a Glass Electrode. *Anal. Chim. Acta* **1967**, *38*, 475−488.
(12) Noszál, B.; Szakács, Z. Microscopic Protonation Equilibria of Oxidized Glutathione. *J. Phys. Chem. B* **2003**, *107*, 5074−5080.
(13) Martell, A. E., Smith, R. M., Eds. *Critical Stability Constants*; Plenum Press: New York, 1974−1989.
(14) Szakács, Z.; Hägele, G.; Tyka, R. ^{1}H/^{31}P NMR pH Indicator Series to Eliminate the Glass Electrode in NMR Spectroscopic pKa Determinations. *Anal. Chim. Acta* **2004**, *522*, 247−258.

(15) MestRe-C computer program, Version 3.5.1Beta, http://www.mestrec.com.
(16) Szakács, Z.; Hägele, G. Accurate determination of low pK values by ¹H NMR titration. *Talanta* **2004**, *62*, 819−825.
(17) Davies, C. W. The Extent of Dissociation of Salts in Water. Part X. Dissociation Minima. *J. Chem. Soc.* **1945**, 460−464.
(18) OPIUM computer program, M. Kyvala, I. Lukes, Chemometrics '95, Pardubice, 1995, Book of Abstracts, p 63; http://www.natur.cuni.cz/∼kyvala/opium.html.

(19) Hoult, D. I. Solvent Peak Saturation with Single-Phase and Quadrature Fourier Transformation. *J. Magn. Reson.* **1976**, *21*, 337−347.
(20) De Marco, A. pH Dependence of Internal References. *J. Magn. Reson.* **1977**, *26*, 527−528.